J. Fluid Mech. (1994), *vol.* 274, *pp.* 339–348

Steep solitary waves in water of finite depth with constant vorticity

By J.-M. VANDEN-BROECK

Department of Mathematics and Center for the Mathematical Sciences, University of Wisconsin-Madison, WI 53705, USA

(Received 21 September 1993 and in revised form 3 February 1994)

Solitary waves with constant vorticity in water of finite depth are calculated numerically by a boundary integral equation method. Previous calculations are confirmed and extended. It is shown that there are branches of solutions which bifurcate from a uniform shear current. Some of these branches are characterized by a limiting configuration with a 120° angle at the crest of the wave. Other branches extend for arbitrary large values of the amplitude of the wave. The corresponding solutions ultimately approach closed regions of constant vorticity in contact with the bottom of the channel. A numerical scheme is presented to calculate directly these closed regions of constant vorticity. In addition, it is shown that there are branches of solutions which do not bifurcate from a uniform shear flow.

1. Introduction

Water waves with constant vorticity have been considered by Benjamin (1962), Simmen & Saffman (1985), Shira (1986), Pullin & Grimshaw (1988), Teles da Silva & Peregrine (1988) and others. Benjamin (1962) derived asymptotic solutions for solitary waves of small amplitude. Shira (1986) considered solitary waves in water of infinite depth. Simmen & Saffman (1985) computed periodic waves of finite amplitude in water of infinite depth by a boundary integral equation method. Teles da Silva & Peregrine (1988) used a similar method to compute periodic waves of finite amplitude in water of finite depth. By considering waves of very large wavelength, they obtained approximate solutions for solitary waves. Solitary waves in water of finite depth were also calculated by Pullin & Grimshaw (1988).

In this paper we study further solitary waves with constant vorticity (see figure 1). We solve the problem by a boundary integral equation technique. Our procedure is similar to the one used by Simmen & Saffman (1985), Pullin & Grimshaw (1988) and Teles da Silva & Peregrine (1988). The formulation and the details of the numerical scheme follow closely previous work on solitary waves in the absence of vorticity (Hunter & Vanden-Broeck 1983; Vanden-Broeck 1991; Vanden-Broeck & Dias 1992; Sha & Vanden-Broeck 1993).

As we shall see, the problem can be characterized by the following parameters:

$$\omega = \Omega H/c, \tag{1.1}$$

$$G = gH/c^2, \tag{1.2}$$

$$\alpha = A/H. \tag{1.3}$$

Here g is the acceleration due to gravity counted positive when acting vertically downwards, Ω the constant value of the vorticity, H the depth of the fluid at infinity, c the value of the velocity on the free surface at infinity and A the elevation of the crest

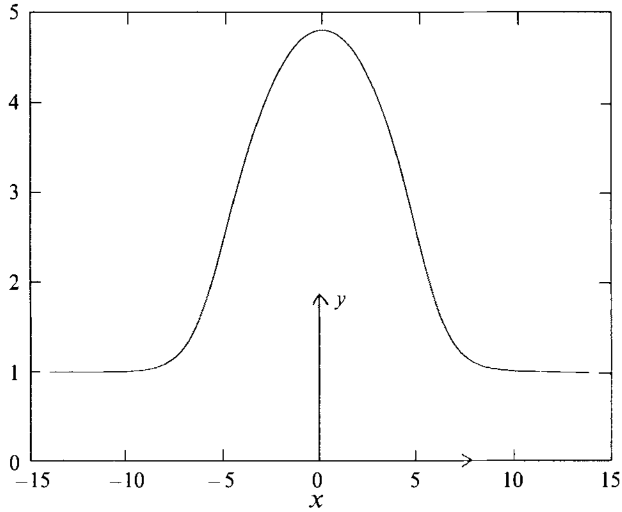

FIGURE 1. Sketch of the flow and of the coordinates. The free surface is a computed solution for $\omega = -0.474$, $A = 3.8$ and $G = 0$.

of the wave on top of the level of the free surface at infinity. The parameter ω is a dimensionless vorticity, G is the dimensionless gravity and α is an amplitude parameter.

The numerical results show that for each value of ω, there is a one-parameter family of solutions which bifurcates from the uniform shear flow at the critical value

$$G = 1+\omega. \tag{1.4}$$

As one progresses along these branches, α increases. For $\omega > \omega_c \approx -0.33$, the wave ultimately reaches a limiting configuration with an 120° angle at its crest. These results agree with those previously obtained by Benjamin (1962) for waves of small amplitude and by Teles da Silva & Peregrine (1988) and Pullin & Grimshaw (1988) for waves of finite amplitude. In particular Benjamin (1962) derived (1.4) by asymptotic methods. For $\omega < \omega_c$, the waves exist for arbitrary large values of α. As $\alpha \rightarrow \infty$, the wave approaches a closed region of constant vorticity in contact with the bottom of the channel along a segment. A numerical procedure is presented to calculate directly these regions of constant vorticity.

We show that for each value of $\omega_c < \omega < 0$, there is an additional family of solutions. Its existence is suggested by the fact that solitary waves with constant vorticity exist in the absence of gravity (i.e. when $G = 0$). As we shall see, they form a one-parameter family of solutions which bifurcates from the uniform shear flow at the critical value $\omega = -1$ (see (1.4)). As one progresses along the branch of solutions, ω increases to zero and α tends to infinity. Therefore for each value of ω between 0 and -1, there is in addition to the branches of solutions which bifurcate from the uniform shear flow an additional solution corresponding to $G = 0$. We show numerically that there is a one-parameter family of solutions which contains the solution with $G = 0$. For $-1 < \omega < \omega_c$, this family coincides with the family of solutions described in the previous paragraph. However for $\omega_c < \omega < 0$, this family is a new family of solutions which does not bifurcate from a uniform shear flow. As one progresses along this branch of solutions, the waves evolve between two limiting configurations. The first limiting configuration is a wave whose profile has one point of contact with itself. The second limiting configuration is again a closed region of constant vorticity in contact with the bottom of the channel.

The problem is formulated in §2. The numerical procedure is described in §3. The numerical results are discussed in §4 and the regions of constant vorticity are computed in §5.

2. Mathematical formulation

We consider a two-dimensional solitary wave in an inviscid incompressible fluid. The fluid is bounded below by a horizontal bottom. The flow is assumed to be rotational and characterized by a constant vorticity Ω. We take a frame of reference with the x-axis along the horizontal bottom and in which the flow is steady. We assume that the flow is symmetric with respect to the y-axis (see figure 1).

We denote by H the depth at infinity and by c the velocity on the free surface at infinity. The variables are made dimensionless by choosing H as the unit length and c as the unit velocity. The flow is described in terms of a stream function $\psi(x,y)$ satisfying

$$\nabla^2\psi = -\omega \tag{2.1}$$

in the flow domain. Here ω is defined in (1.1).

We reduce the problem to one for Laplace's equation by subtraction of a particular solution of (2.1). Thus if we write

$$\psi = \Psi - \tfrac{1}{2}\omega y^2 + (1+\omega)y \tag{2.2}$$

then $\nabla^2\Psi(x,y) = 0$. Now the quantity $w(z) = u - \mathrm{i}v = \Psi_y + \mathrm{i}\Psi_x$ is an analytic function of $x+\mathrm{i}y$, where the fluid velocity vector is $(u-\omega(y-1)+1), v)$. We satisfy the kinematic condition $v = 0$ on the bottom by reflecting the flow in the bottom. The function $w(z)$ vanishes at infinity. Hence by Cauchy's theorem, when z is on the free surface

$$w(z) = -\frac{1}{\pi \mathrm{i}}\oint_C \frac{w(\zeta)\,\mathrm{d}\zeta}{\zeta - z}, \tag{2.3}$$

with a Cauchy principal-value interpretation. Here C denotes the free surface and its image in the bottom.

Suppose that the free surface is parametrized by $x = X(t)$, $y = Y(t)$ where t is the arclength with $t = 0$ at the crest of the wave. Then

$$X'(t)^2 + Y'(t)^2 = 1, \tag{2.4}$$

$$X(0) = 0, \quad Y(0) = 1+\alpha, \tag{2.5}$$

where α is the amplitude parameter defined in (1.3). We now consider u and v to be functions of t. Taking the real part of (2.3) and using the symmetry of the wave with respect to the y-axis, we obtain, after some algebra,

$$\begin{aligned}
\pi u(t) = {} & -\int_0^\infty \frac{(X(s)-X(t))(u(s)\,Y'(s)-v(s)\,X'(s))-(Y(s)-Y(t))(u(s)\,X'(s)+v(s)\,Y'(s))}{(X(s)-X(t))^2+(Y(s)-Y(t))^2}\,\mathrm{d}s \\
& -\int_0^\infty \frac{(X(s)+X(t))(u(s)\,Y'(s)-v(s)\,X'(s))+(Y(t)-Y(s))(u(s)\,X'(s)+v(s)\,Y'(s))}{(X(s)+X(t))^2+(Y(s)-Y(t))^2}\,\mathrm{d}s \\
& +\int_0^\infty \frac{(X(s)-X(t))(v(s)\,X'(s)-u(s)\,Y'(s))+(Y(s)+Y(t))(u(s)\,X'(s)+v(s)\,Y'(s))}{(X(s)-X(t))^2+(Y(s)+Y(t))^2}\,\mathrm{d}s \\
& +\int_0^\infty \frac{(X(s)+X(t))(v(s)\,X'(s)-u(s)\,Y'(s))+(Y(s)+Y(t))(u(s)\,X'(s)+v(s)\,Y'(s))}{(X(s)+X(t))^2+(Y(s)+Y(t))^2}\,\mathrm{d}s,
\end{aligned} \tag{2.6}$$

an equation that holds for all $0 < t < \infty$.

On the free surface, the kinematic condition and Bernoulli equation yield

$$(u+\omega+1-\omega Y)\,Y'(s) = vX'(s), \tag{2.7}$$

$$[u+1-\omega(Y-1)]^2+v^2+2GY = 1+2G. \tag{2.8}$$

Here G is the gravity parameter defined in (1.2). Equation (2.8) expresses the fact that the pressure is constant on the free surface.

For given values of ω and α we seek four functions u, v, X' and Y' satisfying (2.4), (2.6)–(2.8). The parameter G is found as part of the solution.

3. Numerical procedure

We seek a numerical solution of the nonlinear integro-differential system (2.4), (2.6)–(2.8). First we define N distinct mesh points on the free surface by specifying values of the arclength parameter $t = S_I$, where

$$S_I = E(I-1), \quad I = 1, \dots, N. \tag{3.1}$$

Here E is the interval of discretization. We shall also make use of the intermediate mesh points $S_{I-\frac{1}{2}} = \frac{1}{2}(S_{I+1}+S_I)$, $I = 1, 2, \dots, N-1$.

We now define the $4N$ corresponding fundamental unknown quantities

$$u_I = u(S_I), \quad I = 1, 2, \dots, N, \tag{3.2}$$

$$v_I = v(S_I), \quad I = 1, 2, \dots, N, \tag{3.3}$$

$$X'_I = X'(S_I), \quad I = 1, 2, \dots, N, \tag{3.4}$$

and

$$Y'_I = Y'(S_I), \quad I = 1, 2, \dots, N. \tag{3.5}$$

We estimate the values of the x- and y-coordinates $X_I = X(S_I)$, $Y_I = Y(S_I)$ in terms of the fundamental unknowns by the trapezoidal rule, i.e. $X_1 = 0$, $Y_1 = 1+\alpha$ and

$$X_I = X_{I-1}+X'(S_{I-\frac{3}{2}})\,E, \quad I = 2, 3, \dots, N, \tag{3.6}$$

$$Y_I = Y_{I-1}+Y'(S_{I-\frac{3}{2}})\,E, \quad I = 2, 3, \dots, N, \tag{3.7}$$

where $X'(S_{I-\frac{3}{2}})$ and $Y'(S_{I-\frac{3}{2}})$ are evaluated from X'_I and Y'_I by a four-point interpolation formula. We satisfy (2.7) and (2.8) at the mesh points S_I, $I = 1, 2, \dots, N-1$ and (2.4) at the mesh points S_I, $I = 1, 2, \dots, N$. This yields $3N-2$ nonlinear equations. Next we evaluate $X(S_{I-\frac{1}{2}})$, $Y(S_{I-\frac{1}{2}})$ by four-point interpolation.

We then satisfy (2.6) at the point $t = S_{I-\frac{1}{2}}$, $I = 1, 2, \dots, N-1$ by applying the trapezoidal rule to (2.7), with a sum over the points $s = S_J$, $J = 1, 2, \dots, N$. The symmetry of the discretization and of the trapezoidal rule with respect to the singularity of the integrand at $s = t$ enables us to evaluate this Cauchy principal value integral by ignoring the singularity, with an accuracy no less than a non-singular integral. This yields $N-1$ extra nonlinear equations.

Four more equations are obtained by imposing the symmetry condition

$$Y'_1 = 1 \tag{3.8}$$

and the far-field conditions

$$Y_N = 0, \tag{3.9}$$

$$u_N = 0, \tag{3.10}$$

$$v_N = 0. \tag{3.11}$$

We now have $4N+1$ equations for the $4N+1$ unknowns (3.2)–(3.5) and G. This system is solved by Newton's method for given values of α and ω. To obtain the results presented in the next section, we also use a variation of the scheme in which we fix G and ω and find α as part of the solution.

4. Discussion of results

We used the numerical scheme of §3 to compute solutions for various values of ω and α. Most calculations were performed with $N = 150$ and $E = 0.5$. For waves close to the limiting configuration with a 120° angle, we used $E = 0.1$ and $N = 150$ to resolve the sharp crests. In all cases we checked that the numerical results are independent of E and N within graphical accuracy.

Numerical values of α versus G are shown in figure 2 for various values of ω. For all values of ω and G, the uniform shear flow, $\alpha = 0$, $u = 0$, $v = 0$, $X' = 1$ and $Y' = 0$, is a trivial solution. This branch of trivial solutions corresponds to the G-axis in figure 2. The solitary waves are branches of solutions which bifurcate from this trivial solution at the critical values (1.4). Benjamin (1962) derived an asymptotic solution for small values of α. In particular he obtained the following relation among G, α and ω (see his equation (46)):

$$G = 1+\omega-\alpha(1+\omega+\tfrac{1}{3}\omega^2). \tag{4.1}$$

Our numerical values agree with (4.1) as α approaches zero.

As we progress along the branches of solutions, we find that there is a critical value $\omega_c \approx -0.33$ of ω such that different limiting configurations occur for $\omega < \omega_c$ and for $\omega > \omega_c$. For $\omega > \omega_c$, the limiting configuration is characterized by a stagnation point at the crest with a 120° angle. Using (2.8), we find that these limiting configurations satisfy

$$\alpha = 1/(2G). \tag{4.2}$$

Relation (4.2) corresponds to the broken line in figure 2. These branches of solutions have been studied before by Pullin & Grimshaw (1988) and Teles da Silva & Peregrine (1988). In the particular case $\omega = 0$, the solutions agree with previous numerical calculations for solitary waves in the absence of vorticity (see Hunter & Vanden-Broeck 1983 and the references mentioned in that paper). Typical profiles are shown in figures 3(*a*) and 3(*b*).

For $\omega < \omega_c$, the branches of solutions in figure 2 extend for arbitrary large values of α without intersecting the broken curve. As $\alpha \to \infty$, the wave approaches a closed region of constant vorticity in contact with the bottom of the channel. We shall consider further these limiting configurations at the end of this section and in §5. A typical profile for $\omega < \omega_c$ is shown in figure 3(*c*).

Figure 2 shows that there are solitary waves with constant vorticity in the absence of gravity (i.e. $G = 0$). These solutions form a one-parameter family of solutions. Numerical values of α versus ω for $G = 0$ are shown in figure 4. There is again a trivial solution corresponding to a uniform shear flow. This trivial solution corresponds to the ω-axis in figure 4. The solitary waves bifurcate from this trivial solution at $\omega = -1$. A typical free surface profile is shown in figure 1. As $\alpha \to \infty$, $\omega \to 0$ and the wave approaches a circular region made up of fluid in rigid-body rotation and in contact with the bottom of the channel at one point. Such a configuration was suggested by Teles da Silva & Peregrine (1988) as a possible limiting configuration for solitary waves without gravity.

The branches of solutions for $-1 < \omega < \omega_c$ in figure 2 intersect the α-axis. The

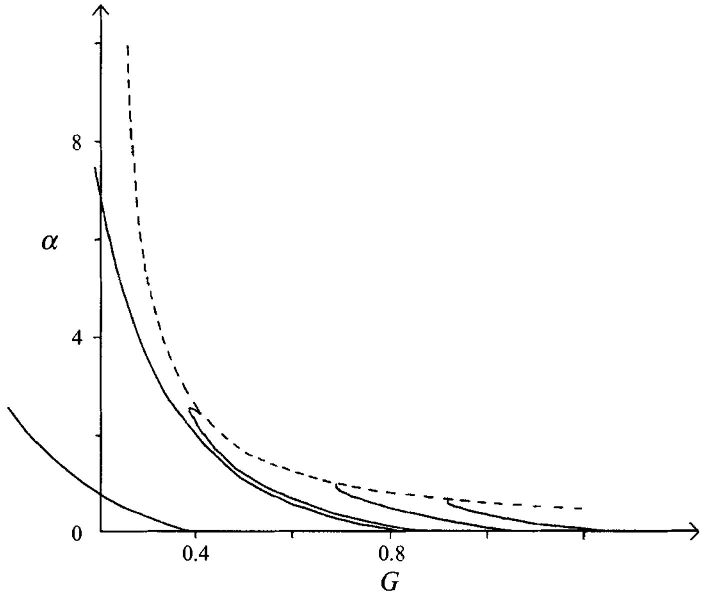

FIGURE 2. Values of α versus G for various values of ω. The curves from right to left correspond to $\omega = 0.11$, -0.11, -0.32, -0.35 and -0.8. The broken curve corresponds to (4.2).

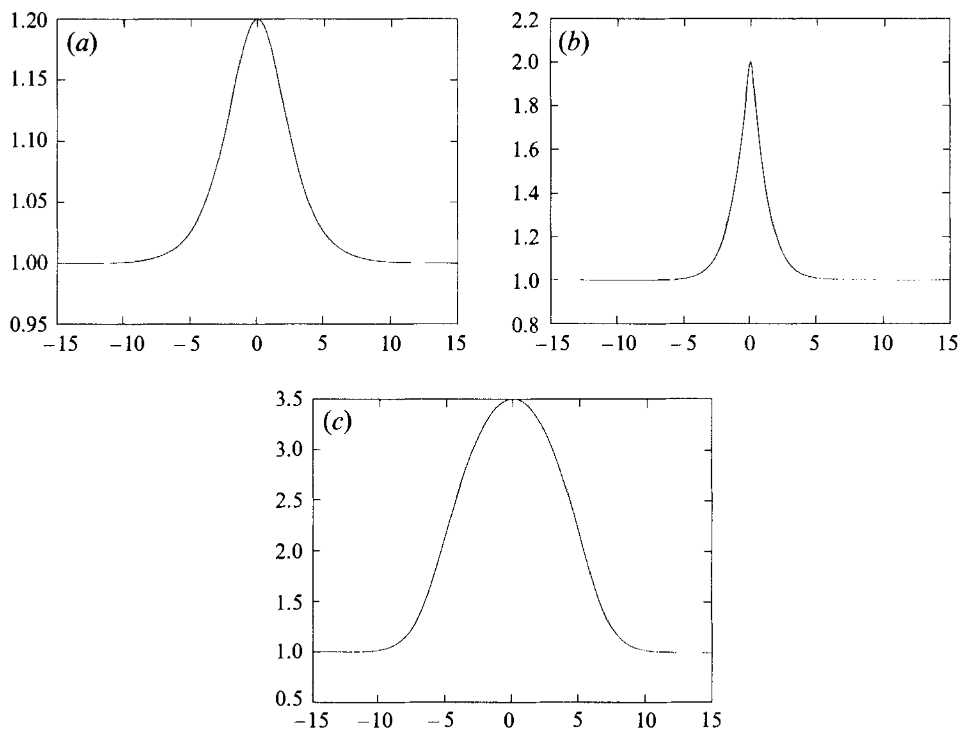

FIGURE 3. Computed free surface profile for (*a*) $\omega = -0.11$, $A = 0.2$ and $G = 0.742$; (*b*) $\omega = -0.11$, $A = 1.0$ and $G = 0.49$ (this solution is closed to the limiting configuration with a 120° angle at the crest); (*c*) $\omega = -0.8$, $A = 2.5$ and $G = -0.19$.

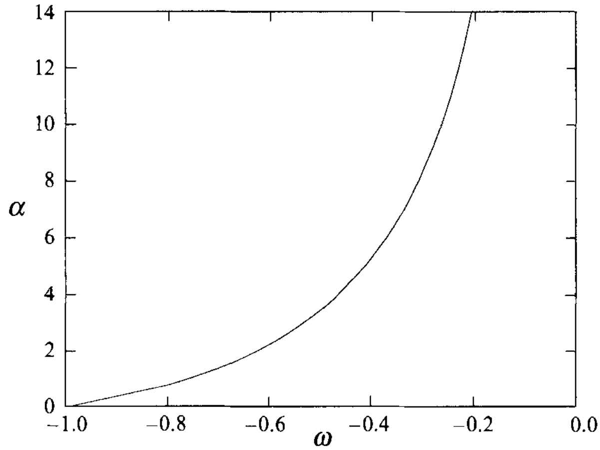

FIGURE 4. Values of α versus ω for solitary waves without gravity.

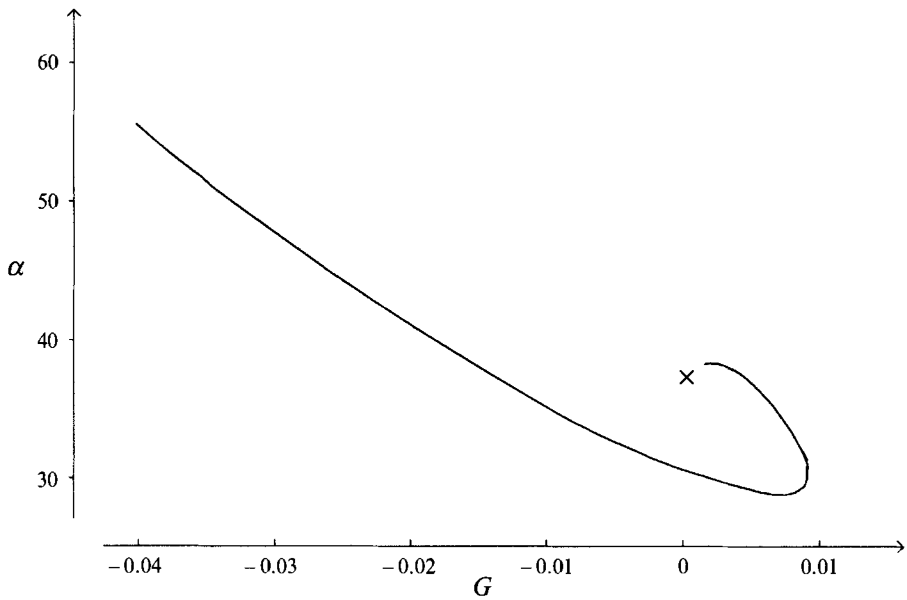

FIGURE 5. Values of α versus G with $\omega = -0.11$ for the new family of waves. The cross corresponds to the solution (4.3).

corresponding solutions are the solutions without gravity of figure 4. For $\omega_c < \omega < 0$, the branches of solutions of figure 2 do not intersect the α-axis and the solutions without gravity are members of a new branch of solutions. These branches were computed by continuation: we used the solution without gravity as the initial guess to compute a solution for a small value of G. This solution was then used as the initial guess to compute a solution for a larger value of G and so on. Values of α versus G for the new branch corresponding to $\omega = -0.11$ are shown in figure 5. Typical free surface profiles are shown in figures 6(a–d). The new branches do not bifurcate from the uniform shear flow and evolve between two different limiting configurations.

The first limiting configuration is a wave whose profile has a point of contact with itself (see figure 6a). It is a wave without gravity (i.e. $G = 0$) and the closed region is

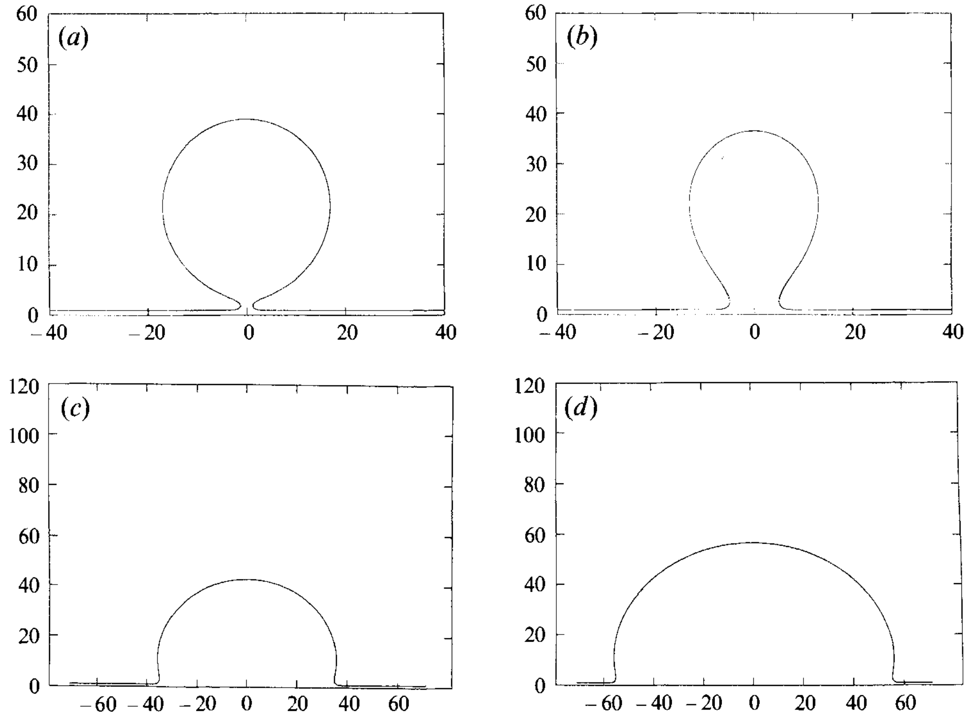

FIGURE 6. Computed free surface profile for (*a*) $\omega = -0.11$, $A = 38$ and $G = 0.0016$; (*b*) $\omega = -0.11$, $A = 35.5$ and $G = 0.0064$; (*c*) $\omega = -0.11$, $A = 41.5$ and $G = -0.02$; (*d*) $\omega = -0.11$, $A = 50.5$ and $G = -0.034$.

again a circular domain made up of fluid in rigid-body rotation. The radius of the circular domain is $\frac{1}{2}A$. Since the velocity on the free surface is 1 when $G = 0$, we have

$$A = -4/\omega. \tag{4.3}$$

For $\omega = -0.11$, (4.3) gives $A = 36.364$. This value corresponds to the cross in figure 5. It is consistent with our numerical calculations.

The second limiting configuration is the same as for the branches of solutions with $\omega < \omega_c$ in figure 2. It is a closed region of constant vorticity in contact with the bottom of the channel along a segment. The approach to this limiting configuration is apparent in figures 6(*c*) and 6(*d*).

As ω increases, the curve in figure 5 moves upwards. We expect that this curve coalesces into the point $\alpha = \infty$, $G = 0$ as $\omega \to 0$ and that the new solutions do not exist for $\omega > 0$. This is suggested by the fact that the solution corresponding to $G = 0$, $\alpha = \infty$ and $\omega = 0$ has the properties of both the first and the second limiting configuration (i.e. the profile of the wave has a point of contact with itself and is in contact with the bottom). As ω approaches ω_c from above, we expect the new family of solutions to merge with the branches of solutions which bifurcate from a uniform shear flow.

5. Limiting configuration

The results of the last section show that there are solitary waves of arbitrary large amplitude. Figures 6(*c*) and 6(*d*) suggest that these waves approach closed regions of constant vorticity touching the bottom along a segment as $\alpha \to \infty$. These closed regions are difficult to calculate accurately by using the scheme of §3, because more and more

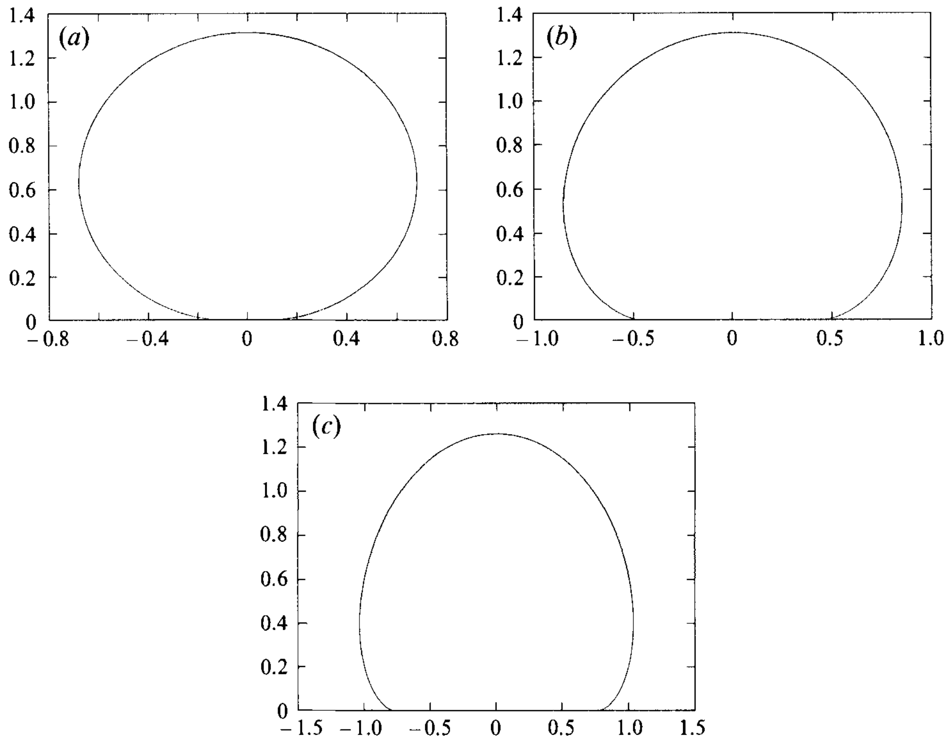

FIGURE 7. Computed solution for a closed region of constant vorticity in contact with a wall with (*a*) $\mu = -0.045$ and $\zeta = 3.04$; (*b*) $\mu = -0.6$ and $\zeta = 3.33$; (*c*) $\mu = -0.21$ and $\zeta = 4.34$.

mesh points are needed on the free surface as α increases. Therefore we shall calculate directly these limiting configurations (see figure 7*a*). We first rescale the variables by choosing the velocity Q at the separation points (i.e. the extremities of the segment of contact) as the unit velocity and the unit length L such that the total length of the free surface is equal to 4. We choose Cartesian coordinates with the origin in the middle of the segment of contact. Then the problem is characterized by the dimensionless gravity and the dimensionless vorticity

$$\mu = 2gL/Q^2, \tag{5.1}$$

$$\zeta = \Omega L/Q. \tag{5.2}$$

Following the formulation of §2 and Vanden-Broeck & Tuck (1994), we introduce the stream function ψ and write

$$\psi = \Psi - \tfrac{1}{2}\zeta y^2; \tag{5.3}$$

then $\nabla^2\Psi(x,y) = 0$. As in §2, $w(z) = u - \mathrm{i}v = \Psi_y + \mathrm{i}\Psi_x$ is an analytic function of $z = x + \mathrm{i}y$, where the fluid velocity is now $(u - \zeta y, v)$. We parametrize the free surface by $x = X(t)$, $y = Y(t)$ where t is the arclength with $t = 0$ at the left separation point. Then $X'(t)$ and $Y'(t)$ satisfy (2.4) and $X(2) = 0$. Proceeding as in §2, we find that the integro-differential equation (2.6) still holds with the upper limit ∞ replaced by 2.

On the free surface, the kinematic condition and Bernoulli equation yield

$$(u - \zeta Y)\, Y'(s) = vX'(s), \tag{5.4}$$

$$(u - \zeta Y)^2 + v^2 + \mu Y = 1. \tag{5.5}$$

This completes the formulation of the problem. For a given value of μ we seek four functions u, v, X' and Y' satisfying (2.4), (2.6), (5.4) and (5.5). The value of ζ is found as part of the solution.

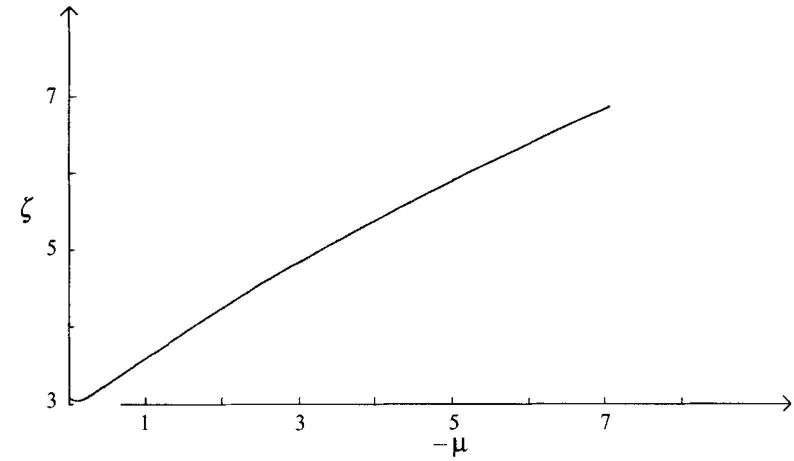

FIGURE 8. Values of ζ versus $-\mu$.

We solved the problem numerically by using a numerical procedure similar to the one described in §3. Most of the numerical results were obtained with 60 equally spaced mesh points between $s = 0$ and $s = 2$.

Typical free surface profiles are shown in figure 7(*a–c*). For $\mu = 0$, the solution is a circular region of fluid in rigid-body rotation with one point of contact with the bottom. The corresponding value of ζ is π. A graph of ζ versus $-\mu$ is shown in figure 8. We found that there is a solution for each value of $\mu < 0$. As μ becomes more negative, ζ increases and the length of the segment of contact increases.

Vanden-Broeck & Tuck (1994) considered closed regions of constant vorticity in contact with curved boundaries. The results of this section generalize some of their findings by including the effect of gravity.

This work was supported by the National Science Foundation.

REFERENCES

BENJAMIN, T. B. 1962 The solitary wave on a stream with an arbitrary distribution of vorticity. *J. Fluid Mech.* **12**, 97–116.

HUNTER, J. K. & VANDEN-BROECK, J.-M. 1983 Accurate computations for steep solitary waves. *J. Fluid Mech.* **136**, 63–71.

PULLIN, D. I. & GRIMSHAW, R. H. J. 1988 Finite amplitude solitary waves at the interface between two homogeneous fluids. *Phys. Fluids* **31**, 3550–3559.

SHA, H. & VANDEN-BROECK, J.-M. 1993 Two layer flows past a semicircular obstruction. *Phys. Fluids* A **5**, 2661–2668.

SHIRA, V. I. 1986 Nonlinear waves at the surface of a liquid layer with a constant vorticity. *Dokl. Acad. Nauk.* **286**, 1332–1336.

SIMMEN, J. A. & SAFFMAN, P. G. 1985 Steady deep water waves on a linear shear current. *Stud. Appl. Maths* **73**, 35–57.

TELES DA SILVA, A. F. & PEREGRINE, D. H. 1988 Steep surface waves on water of finite depth with constant vorticity. *J. Fluid Mech.* **195**, 281–302.

VANDEN-BROECK, J.-M. 1991 Elevation solitary waves with surface tension. *Phys. Fluids* A **3**, 2659–2663.

VANDEN-BROECK, J.-M. & DIAS, F. 1992 Gravity-capillary solitary waves in water of infinite depth and related free-surface flows. *J. Fluid Mech.* **240**, 549–557.

VANDEN-BROECK, J.-M. & TUCK, E. O. 1994 Steady inviscid rotational flows with free surfaces. *J. Fluid Mech.* **258**, 105–113.